ORIGINAL PAPER

Assessing Long-Term Excavation Damage in Switzerland's Bedretto Adit: A Field Investigation in the Northern Section

**Rodrigo Alcaino-Olivares ·
Chrysothemis Paraskevopoulou [ID] ·
Matthew A. Perras**

Abstract The Bedretto adit, in the Alps of Switzerland, was excavated in 1972–1982 as an auxiliary adit for the main Furka Base Tunnel. The adit is 5218 m long, being excavated mostly in the Rotondo Granite with drill and blast methods to create a horseshoe cross-section. Much of the tunnel has remained unlined and such long observation periods are seldom available since tunnels typically are lined shortly after construction and mines are often closed or backfilled. Previous research in 2004 characterized the depth of failure (DoF) around the adit and found on average a depth of 1.1 ± 0.03 m. A site investigation was carried out in 2017, aimed to measure the DoF through 3D light detection and ranging scanned sections again. The new 3D scans covered a longer section of the tunnel with each scan, up to 6 m in length, compared to the previous laser scans with a single circumferential pass. The results were compared with the data from 2004 and with empirical and numerical prediction curves for Excavation Damage Zone depths. The findings indicate that between 2004 and 2017, the measured DoF generally extended, on average, by 0.1 m, implying that failure has progressed with time. Furthermore, the analysis showed that the volume of failure from 2004 extended up to 1.9 m^3/m, and this volume increased to 3.2 m^3/m in 2017 on average. The VoF was used as a means to overcome the challenge of comparing past to present scan results, since the exact location of the 2004 measurements were not known. Significant variations in the measured DoF at sections of the adit near faults and below a glacier indicate that these external factors can significantly influence the rock mass behaviour. When comparing the DoF to empirical excavation damage zone prediction intervals, the level of damage at the Bedretto adit is comparable with the outer excavation damage zone. This is a region of isolated micro-cracking, and it conceptually suggests that the continued spalling in the Bedretto adit is the results of crack propagation from initial excavation induced damage that leads to interaction even after 41 years since excavation works ceased.

Keywords Long-term brittle rock behaviour ·
Spalling · Brittle damage · Crack propagation

R. Alcaino-Olivares · C. Paraskevopoulou (✉)
School of Earth and Environment, University of Leeds,
Woodhouse, Leeds LS2 9JT, UK
e-mail: c.paraskevopoulou@leeds.ac.uk

R. Alcaino-Olivares · M. A. Perras
Department of Civil Engineering, York University, 4700
Keele, Toronto, ON M3J 1P3, Canada

M. A. Perras
Department of Earth Sciences, ETH Zurich, 5
Sonneggstrasse, 8092 Zurich, Switzerland

1 Introduction

Underground excavations produce changes in the local tangential stress at the excavation surface. In

brittle, hard rock environments, when the magnitude of this local stress concentration exceeds the intact rock crack initiation (CI) threshold, stress-induced spalling or slabbing begins to occur, as observed, and documented by many authors (Martin et al. 1997, 1999; Diederichs 2007; Andersson and Martin 2009; Martin and Christiansson 2009; Perras and Diederichs 2016; Boon 2022). Diederichs (2007) defined spalling as "the development of visible extension fractures under compressive loading". These fractures can range from minor surficial fracturing to spalling damage triggering strain bursting (i.e. progressive failure related to sudden energy release), as reported by many authors (i.e. Duan et al. 2019; Keneti and Sainsbury 2020; Zhang et al. 2020a, b; Askaripour et al. 2022; Aujmaya et al. 2022; Zhao et al. 2022; Zhao et al. 2023; Chiwara et al. 2023). Depending on the stress magnitude, orientation, and tunnel design (size and shape), a "V-shaped notch" can be formed, as it has been observed and described by Martin et al. (1997). The V-shape may not be well developed if the spalling process breaks back and interacts with existing geological structures around the tunnel, as the interaction will change the stress concentrations and result in an asymmetric damage region (Ortlepp and Stacey 1994; Zhang et al. 2012). Although this has not been documented explicitly by many authors at the excavation scale recently, the interaction of geological structures with spalling and rock bursting have been documented by many authors, such as Zhou et al. 2015; Li et al. 2021a, b; and Guo et al. 2023 to name a few, and more recently it has been studied at the laboratory scale (e.g. Pan et al. 2020; Xue et al. 2023) and documented in-situ by Wu et al. (2023 and references therein). The spall geometry development can be described in three stages in an unlined tunnel:

1. Initiation occurs when the micro-cracks near the tunnel face have been closed, and new cracks are being generated.
2. Preferential growth and crack interaction, with crack growth caused by crushing in localised zones with slabbing and spalling on the zone's flank, guided by increasing the tangential stress at the zone tip due to the tunnel face advancing.
3. Stabilisation, at which point the notch's geometry and the tangential stresses stabilise the flanks and

the modified orientation of the principal stresses increases the confinement to prevent continued crack growth at the zone tip.

Whilst the spalling process develops, thin rock slabs will form parallel to the failed zones' surface and be influenced by pre-existing structures that can control the final spalled region's shape. Once this initial failure process has stabilised and stress relaxation is achieved, other factors can contribute to long-term crack growth, and such factors could influence the progressive failure of individual layers (Paraskevopoulou et al. 2015a, b, 2017). They can include gravitational forces, stress corrosion or pressure from deeper layers within the rock mass walls. Additionally, the surrounding faults contribute to the tunnel damage (expand beyond typical spalled depth) and deformation by triggering displacements due to the often-weak nature of the fault rocks, however, moving away from the fault deformations tend to decrease therefore the stress change near the fault influences spalling (Zhang et al. 2019). These factors can lead to slabs failing from the spalled zones long after the tunnel's construction is completed if rock support is not installed to hold it up or continued crack growth (Martin et al. 1999; Jiang et al. 2019; Zhang et al. 2020a, b; Innocente et al. 2022; Zhao et al. 2022), indicating that spalling in brittle rocks can be a time-dependent process. Although these studies have indicated and observed time-dependent damage around underground excavation, they have only documented several months to one year of damage evolution. The study presented here in may well be the longest recorded field observations of spalling damage with time, spanning almost 35 years since the excavation was completed to the date of the last field measurements that record increases in the spalling depth with time.

1.1 Determining the Depth of Brittle Spalling

Aiming to determine the conditions and extension or depth of the spalls, several authors have followed approaches from extensional-strain theory to cohesion loss and friction mobilisation, using laboratory scale spalling tests, development of analytical equations and field observations, as summarized by Barton and Shen (2017). The authors claim that the stress-strength ratio is directly related to brittle failure in underground

excavations as studied not only by the authors, but also documented empirically by Martin et al. (1999); Diederichs (2007); Diederichs et al. 2010; Perras and Diederichs (2016). In fact, it is pointed out that Martin et al. (1999) achieved the best fit for a failure initiation criterion by the definition of a linear relationship between the stress-strength ratio, using Unconfined Compressive Strength, and the depth of failure (DoF) to predict the over-break depth of brittle failure around tunnels. The stress-strength ratio is defined as the quotient between the maximum tangential stress near the adit surface (σ_{max} in Eq. 1 for circular sections) and the uniaxial compressive strength (UCS) of the intact rock. For a circular tunnel, the DoF is the quotient between the radius of failure (r) over the original design radius (R) of an underground excavation, both measured from the centre of the excavation, as mathematically detailed in Eq. (2).

$$\sigma_{max} = 3\sigma_1 - \sigma_3 \qquad (1)$$

$$DoF = \frac{r}{R} = 1.25 * \frac{\sigma_{max}}{UCS} + 0.49 \qquad (2)$$

The empirical correlation from Martin et al. (1999) was derived from in-situ observations conducted among various underground projects. Most of the spalling was observed in tunnels where external factors away from the tunnel were not documented to influence the spall regions shape, such as joints, faults, or geological formation boundaries. Additionally, the quotient between vertical and horizontal stresses across all the case studies when it is above one requires stress concentration at one location around the excavation to initiate the spalling process. Continued efforts have been made to add more case studies to this spalling database to expand to include other environments and associated with other rock types and stress scenarios. Diederichs (2007) expanded the empirical database and related the stress-strength ratio to the CI threshold, which has been well documented to be related to the wall strength around underground excavations in brittle rocks. Following this work, Perras and Diederichs (2016) demonstrated numerical that a non-linear stress-strength relationship better captures the relationship when compared to more empirical evidence at higher stress-strength ratios. The numerically derived damage depth prediction curves were compared to the in-situ measurements of the DoF of the Excavation Damage Zones (EDZ) regions. The EDZ are a group of several annular regions around the excavation, as shown in Fig. 1a. The non-linear depth to the outer bound of the different EDZ regions around a circular tunnel is plotted in Fig. 1b, according to Perras and Diederichs (2016). The description of the EDZ regions is based on the radius of failure (r) and radius of the designed
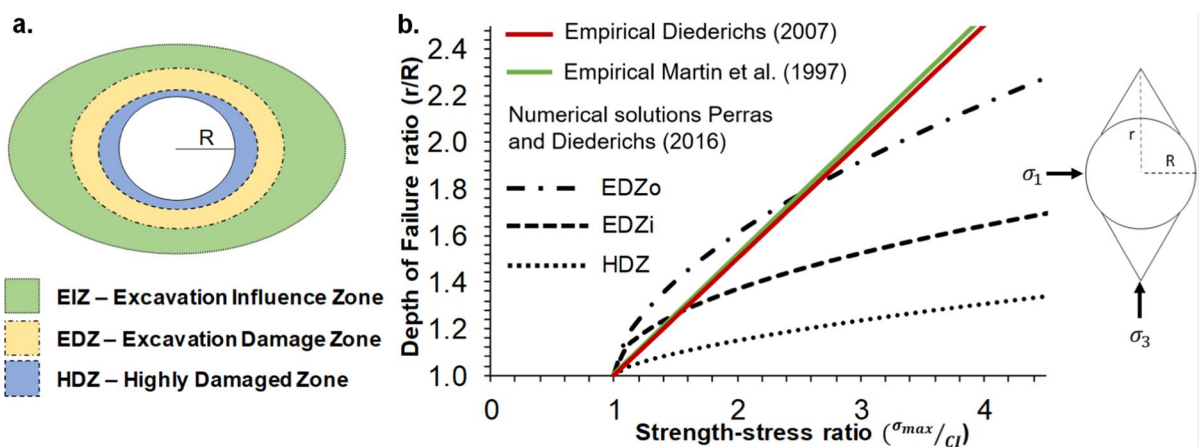

Fig. 1 Different damage zones and **a** an illustration of how they progress away from a circular tunnel surface and **b** numerically derived predictions intervals (95%) for the HDZ, EDZi and EDZo (after Perras and Diederichs 2016), in comparison with linear empirical depth of failure presented by Diederichs (2003) and Martin et al. (1999), as a function of the ratio of maximum stress around a circular excavation ($\sigma_{max} = 3\sigma_1 - \sigma_3$, Eq. 1) to the crack initiation stress value (CI)

excavation (R), (Fig. 1b), EDZ is classified then as follows:

- Highly Damaged Zone (HDZ), associated with the interconnection of macro-fractures.
- Excavation Damaged Zone (EDZ), which is a transition from open and dilated cracks in the inner annular section (EDZi) to isolated micro-cracks with no dilation at the outer edge (EDZo).
- Excavation Influence Zone (EIZ), where only elastic deformations are expected.

Our team aimed to contribute to the DoF dataset, and its relationship proposed by Perras and Diederichs (2016), so the present research is focused on providing field observation and measurement results for the DoF of the unlined Bedretto tunnel (Switzerland) and providing a qualitative discussion of the DoF and EDZ relationship derived from the acquired data.

1.2 Challenges with Time-Dependent Brittle Spalling Depth Data Collection

Potyondy (2007) once said that there is lack of relevant data available to validate time-dependent models for brittle rock behaviour. Although research at the laboratory scale on a variety of rock types has been conducted by a variety of researchers ((e.g. Brantut et al. 2014; Nara et al. 2014; Paraskevopoulou et al. 2017; Paraskevopoulou et al. 2018; Xue et al. 2023) and many authors have developed numerical modelling approaches that capture the laboratory or crustal scale brittle behaviour (see Xue et al. 2023 for a thorough discussion), there is lack of observations of time-dependent damage evolution at the excavation scale to generate validate such models against. Although more recently work (Jiang et al. 2019; Zhang et al. 2020a, b; Innocente et al. 2022) has been building on initial observations of time-dependent brittle fracture from Canada's Underground Research Laboratory (Martin et al. 1999), there are still relatively few case studies with time spans of more than a few months to a year avialable in the literature. The present study may well be the longest observation period with quantified results available, although it is not without its challenges.

The specific tasks of the research presented in this paper involved scanning and documenting the unlined walls' over-break depth along the northern 2000 m of the Bedretto adit. At the time, the Bedretto adit was essentially abandoned. Air circulation for the Furka Base tunnel was directed out through the Bedretto adit, but no other services (lighting, transportation) were available during data collection. Portable lights were used for photographing the spalling; however, the use of the LiDAR system did not require lighting and was ideal for scanning the distance from the machine to the wall surface. One challenge with the scanning was that the exact location of former scans by Huber (2004) were only documented at the meter length, but the scan was only collected in a narrow cross-sectional band (centimeters). For comparison, the LiDAR scans of the present study captured a 6 m longitudinal distance and so analysis methods were developed to aid in comparison of the data.

The post-scanning results are linked to Martin et al. (1999) empirical, and Perras and Diederichs (2016) numerical approaches. The observations from this paper have been compared to previous empirical and numerical prediction lines or curves and demonstrate or add to the empirical evidence. The results further add a unique element related to the time-dependent nature of spalling. This is the longest time span that documents a clear increase in the depth of spalling, in a continuous manner after over 35 years from the excavation date. Furthermore, the results are analysed in terms of change with time using both data sets available from 2004 and measured by this team in 2017. Such long-term observations are rarely available, since either the excavation becomes fully lined (tunnelling) or the excavation is closed or backfilled (mining). The unique opportunity to observe and measure time-dependent brittle damage evolution from the Bedretto adit has been documented in this paper. The following sections detail the overall characteristics of the site and the data acquisition process.

2 The Bedretto Adit Site

The Bedretto adit is a tunnel 5218 m in length, which connects the Furka base tunnel to the Bedretto valley at an elevation of about 1475 m.a.s.l., near the village of Bedretto in the Swiss Canton of Ticino approximately 100 km south of Zurich, Switzerland (Fig. 2a). The Furka Base Tunnel and the Bedretto adit were excavated between 1972 and 1982. The Bedretto adit was abandoned

Fig. 2 Geology of the study area showing the location of the Bedretto adit. **a** Large scale map with Gotthard Massif and Aar Massif ranges nearby Bedretto Valley. **b** Exterior landscape satellite image of Bedretto Adit. Tunnels and glacier location are indicated in figure. **c** Geological map of the study area, with main rock types. The study area is between tunnel meter TM-5218 and TM-3200, with the southern portal being TM-0 and the Northern portal connecting with the Furka Base Tunnel. Source: Modified from the Swiss Geological Survey, Geology of Switzerland 1:500 K, 2005
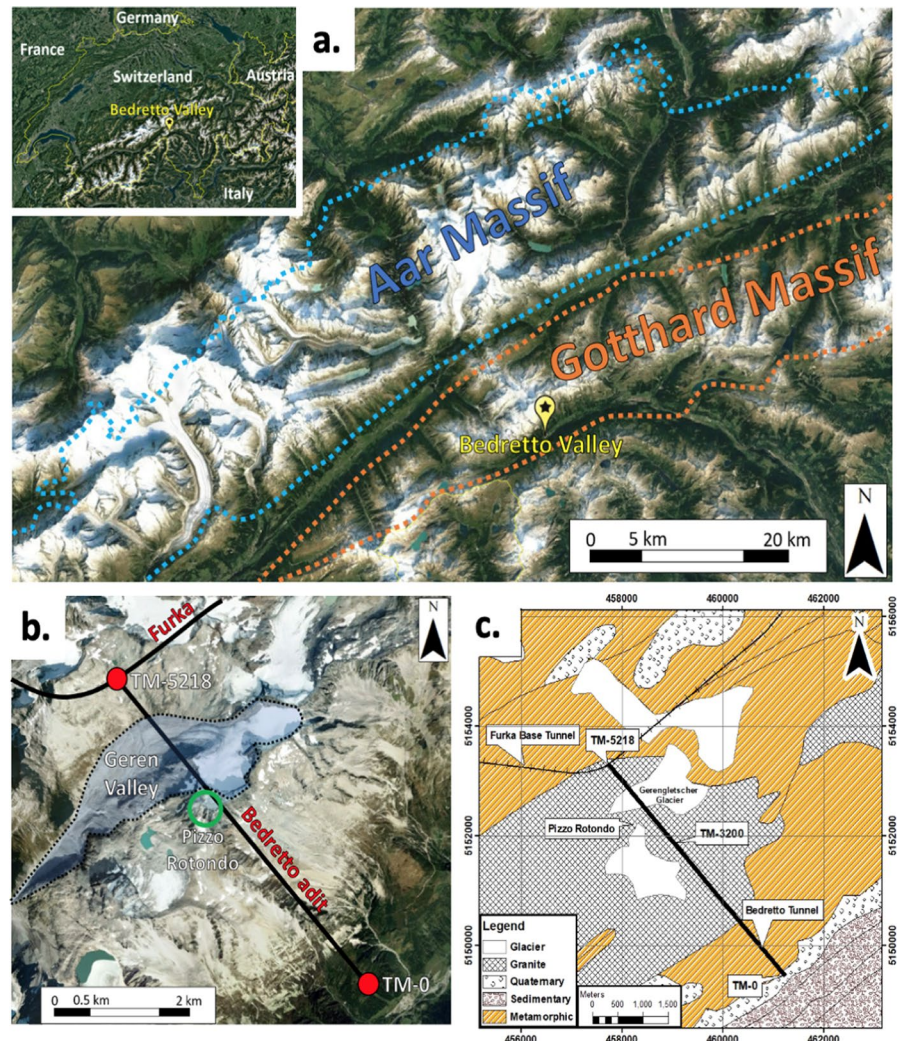
after being used as an auxiliary construction adit for the Furka Base tunnel construction. The adit was excavated by conventional drill and blast techniques with a horseshoe or sometimes a square shape approximately 2.8 m in width and height. The tunnel walls are generally unlined; however, some specific sections, such as fault zones or deep spalled regions, were reinforced with steel arches or mesh and rock bolts for safety purposes. Spalling after adit advance during construction impacted the adit walls' stability (Amberg 1983; Keller and Schneider 1982; Amberg and Sala 1984). The floor is mainly covered by muck, which varies in some sections from crushed rock to sand. However, the walls and roof have remained unlined since construction, and the authors have observed spalling slabs falling off

in recent years. The unlined portions of the adit represent a unique opportunity to observe what damage has occurred since the time of construction (1982). Observations and damage depth measurements were recorded in 2004 in a thesis by Huber (2004) and compared with the authors measurements from 2017. To the authors knowledge, this represents the longest period of time-dependent brittle damage observations in the literature.

2.1 Geological Setting

The morphology above the Bedretto adit is characterised by high mountain ridges with elevations of up to 3200 m and valleys with bottom elevations of about 2500 m. The overburden above the adit ranges up to 1600 m as

the adit passes from the Furka Base Tunnel in the north, under the Gerengletscher glacier on the north flank of the Rotondo Mountain and finally exiting into the Bedretto valley (Fig. 2a), where the overburden gradually diminishes. The adit is in the Gotthard Massif of the Central Alps consisting mainly of Variscan granite (~260 Mio years) and metamorphic rocks, including brittle faults and ductile shear zones that developed during the Alpine orogeny on the European continental crust (Huber 2004; Lutzenkirchen and Loew 2011). Quaternary deposits (debris fans, alluvial infills, landslide deposits and moraines) are observed mainly on the steep slopes and valley infills (TM-0 in Fig. 2b). The Rotondo granite is encountered from TM-5218 to TM-1200, while the adit passes through metamorphic sequences (gneiss and schist) and a deep-seated landslide in the southern section between TM-1200 to TM-0, as shown in Fig. 2c (Ofterdinger et al. 2004).

Four fracture sets have been identified in the Rotondo granite section, generally dipping sub-vertically, with 140/86 SW being the most predominant. Glaciated areas and seasonal snow melting in the mountains above the adit in the Geren Valley (Fig. 2b) area results in water flow through persistent geological structures, down into the Bedretto adit (Amberg 1983). The hydraulic conductivity of the rock mass and the water inflows inside the ad-it are strongly affected by preferential pathways associated with large fault zones and the joint network. Initial inflows along individual fault zones in the granite section of the Bedretto adit were up to 40 l/s (Keller and Schneider 1982; Keller et. al. 1987), but they have decreased substantially in the meantime.

The estimated average vertical stress in the studied sections is 35 MPa, with variations due to topography and glaciers along the adit. The estimated K-ratio (Ko) is roughly 0.7 on average (Huber 2004), but these estimations are much uncertain. A recent geothermal energy project at TM-2000 with an overburden thickness of 1000 m estimated that the vertical stress was approximately 26.5 MPa and Ko ranges from 0.8 to 1.0 (Gischig et al. 2020). Differences between wall conditions (East and West) and the non-symmetrical nature of the failed zones along the adit suggest that the orientation of the principal stresses may be slightly rotated from the vertical and horizontal axes. Since no measurements were taken in the tunnel sections examined in this paper, the higher vertical stress estimate and the lower Ko value will be used, as this will result in higher depths of spall prediction compared to the field measurements. The rock mass's geotechnical properties have been summarised in Table 1, gathered through laboratory tests for Bedretto intact samples on non-weathered slabs from the adit and information collected from granites of the Aar and Gotthard Massifs (Huber 2004; Keller et al. 1987).

2.2 Previous Spalling Observations within the Bedretto Adit

To analyse the over-break depth of the walls 22 years after the end of construction, research conducted in 2004 by Huber (2004) aimed to document the shape of spalled regions between TM-5200 and TM-4600. Their investigation indicated that the geometry and shape of the spalled regions in the Bedretto adit generally fit Martin's empirical DoF correlation (Martin et al. 1999). However, the depth did not agree with the empirical correlation where existing geological structures influence the spalling process. In addition to the DoF analysis, Huber (2004) also provided information about geological structures, rock strength estimated from point load tests (PLT), mineralogy of the rock walls and qualitative observations of the stress-induced failure. The observed qualitative elements of the failure region were reported as:

- Spalled slabs had thicknesses from mm to tens of cm.
- Kink bands formed at the edge of the spalled region and were symmetrically triangular in the order of 5–20 cm.

Table 1 Geotechnical Parameters estimated for the Rotondo Granite

Parameter	Value
Density (ρ)	2700 (kg/m^3)
Tensile strength (σ_t)	5 (MPa)
Unconfined compressive strength (UCS)	120–200 (MPa)
Young's module (E)	20 (GPa)
Poisson's ratio (v)	0.25

The unconfined compres-sive strength (UCS) values were estimated from PLT made by Huber (2004) at intact and non-weathered specimens from the Bedretto Adit

- Kink bands tend to form in areas where structures exist, or bolts were installed prior to spall development.
- Kink bands were not found where classic V-shaped notches developed (typical of spalling in massive granite—see Martin et al. 1997) were not widely observed in the adit, although they were identifiable in some locations (e.g. close to Furka Tunnel at TM-5096).
- Tension cracks associated with spall slabs parallel to the adit wall were found and considered to form during buckling of the spalled slabs.

Our team carried out a field campaign using a LiDAR scanner to determine the existing geometry and calculate the DoF along 500 m of the tunnel, from TM-5120 to TM-4670 as indicated in Fig. 2b, c, in order to gather more spalling depth data and investigate the changes with time from previous measurements from Huber (2004). The field observations and information from the LiDAR scanning conducted by this research team complemented the existing description of the Bedretto adit stability, and conditions are generally like those observed in previous investigations at the site. Visual inspection reveals that spall geometry is still limited by pre-existing structures (joints), as shown in Fig. 3a. Blast holes have been seen frequently in the roof, indicating that the roof is well preserved since construction and that spalling damage continues to be observed in the sidewalls only, as this is related in part to the higher stress concentration in the sidewalls (Fig. 3b). Continued accumulation of slabs is evidence of the ongoing progressive failure of either existing spalled slabs or new spalls (Fig. 3c). This research focuses on the changes recorded in the DoF as measured from the LiDAR scans of the adit in 2017 and compared to the data gathered in 2004.

3 Methodology

A field campaign was conducted to measure the overbreak depth of the tunnel in the same section measured by Huber (2004). The main objective was to scan the tunnel walls from the Bedretto adit and Furka tunnel (TM-5218) intersection towards the adit portal in the Bedretto Valley, up to TM-3200 (Fig. 4a). This task was carried out with a Faro-Focus 3D scanner,
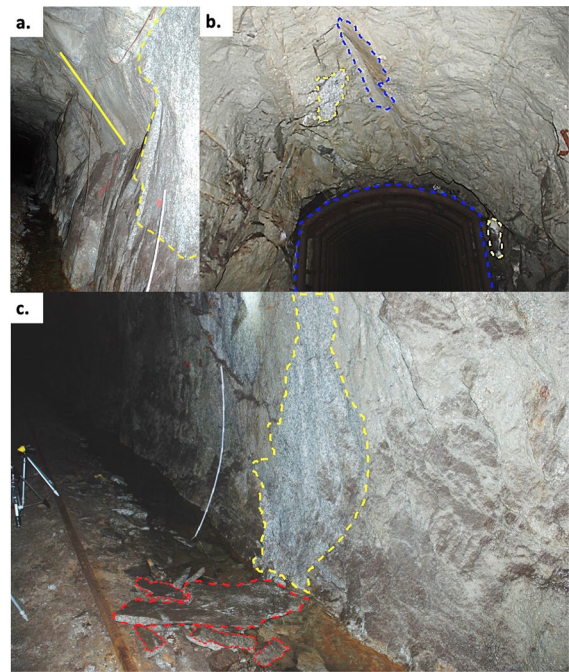

Fig. 3 Evidence of spalling from in Bedretto Adit (Switzerland) during site investigations in 2017. **a** V-shaped notch (solid yellow line) and fresh spalls indicated by the thin slabs of rock in the side wall (outlined in dashed yellow), **b** fresh roof over-break (yellow dashed line) with evidence of a blast-hole (blue dashed line) and steel arches (blue dashed line) in the background used in a fault zone, **c** Fresh side wall spall (yellow dashed line) and fallen rock pieces next to the rail on the invert. Source: Alcaino-Olivares (2017)

with an accuracy of ± 1mm. Over 60 scans were taken at points where either Huber (2004) had measured the DoF or recent spalling activity exposed fresh rock in the adit walls (Figs. 3c and 4b).

The scans were processed in SCENE® (V6.2.4.30 from Faro) for a 3D perspective and to eliminate points which were too erratic or were captured far away from the centre of the scanner (Fig. 4c).

The processed scanned section was then inputted in CloudCompare® to calculate the volumetric differences of failure (VoF) between the scanned (current) and designed (base line) tunnel section by subtracting one to each other. The result was then normalized by the length of the scan section, which was typically 6 m (3m in both directions from the centre). In most scanned sections, the floor had an unknown thickness of muck or sand present, so floors were deleted from the point cloud. The VoF results were used to calculate the DoF of each tunnel section, hence DoF values represent an

Fig. 4 The steps of the scanning and data processing procedure at the Bedretto adit, **a**. Faro Focus Scan setup at the centreline of the adit (example at the Bedretto Valley's portal, TM-0), **b**. Selection of sections to scan, and placement of illumination, **c**. scanned data in SCENE® being cut into a specific section and d. examination of over-break depth and volume in CC® with the bold line showing the original design profile of the Bedretto adit for the purposes of comparison with past scans
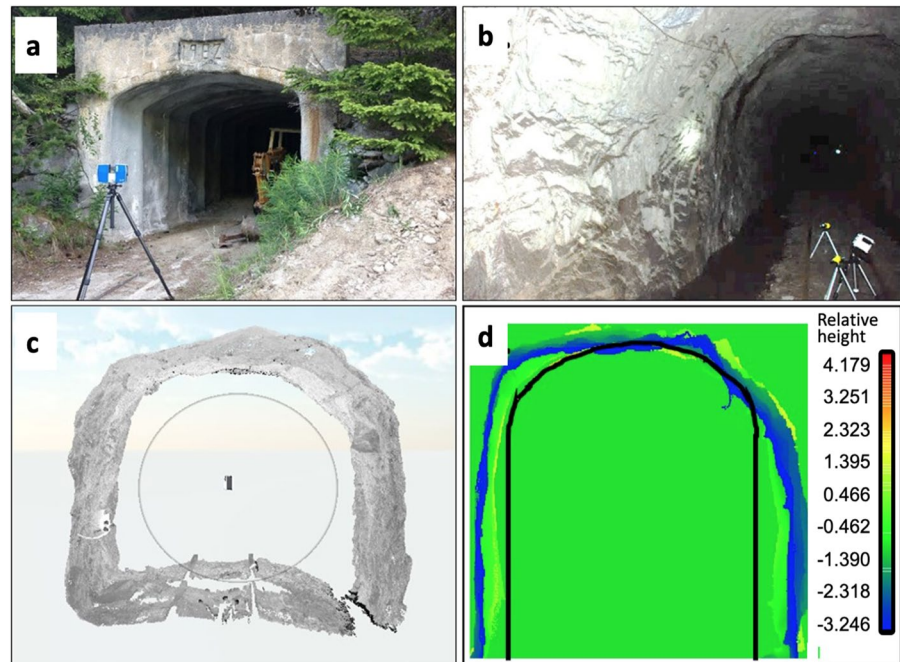
average of the individual tunnel section rather than focusing on the largest over-break values as done by Huber (2004). The DoF was calculated using Eq. (3) from the VoF results to get an average volumetric DoF for the entire scan section. It was assumed that the tunnel's cylindrical geometry with an equivalent circular radius (R) for the Bedretto adit design equals 2.1 m, like Huber's assumption (Huber 2004). Thus, the length of the section (L) is fixed at 6 m, and the average radius of failure (r) as the effective circular radius to the average outer point of failure.

$$DoF = \frac{r}{R} = \sqrt{\frac{VoF}{\pi L R^2} + 1} \qquad (3)$$

4 Lidar Depth of Damage Scanning Results

The raw DoF values from the current study and Huber (2004) data are shown in Fig. 5, plotted along with Martin et al. (1999) empirical correlation for the DoF due to spalling versus stress-strength ratio graph. The expected region was outlined by the green dashed line in Fig. 5, based on locally estimated inputs. The less number samples for Huber (2004) data is due to the authors' study covered only the

500 m at the most northern section of Bedretto (i.e. TM-5120 to TM-4670). In contrast, our field measurements covered from TM-5152 to TM-3280. For both data sets, the stress value varies along the tunnel alignment related to the changes in the overburden thickness which influences the vertical stress and, hence, the maximum stress at the tunnel section. The vertical stress was calculated as influenced by gravity solely (Eq. 4 in MPa, h stands for overburden distance in m), and a horizontal to vertical stress ratio (K) equals to 0.7 (Huber 2004) was used to determine the horizontal stress (Eq. 5). Therefore, the maximum tangential stress (Eq. 1) to strength ratio used in this study changes solely due changes in the over-burden depth and the resulting stress estimated therein, as detailed by Eq. (2). The strength in terms of UCS was fixed at 150 MPa only for the current data, regardless the location across Bedretto. However, Huber (2004) conducted PLT tests to estimate local strength values, which ranged from 120 to 200 [MPa] (see Table 1).

$$\sigma_v = 0.27 * h \qquad (4)$$

$$\sigma_h = K * \sigma_v = 0.7 * \sigma_v \qquad (5)$$

The DoF for Huber (2004) data scatter from 0.75 to 1.28, whilst their stress-strength ratio varies

Fig. 5 Depth of Failure (DoF) values for the Bedretto adit against the stress to strength ratio for the scanned sections from Huber (2004) and the current study data (2017). The green solid line is the average and green dashed line the minimum and maximum empirical relationship according to Martin et al. (1999)
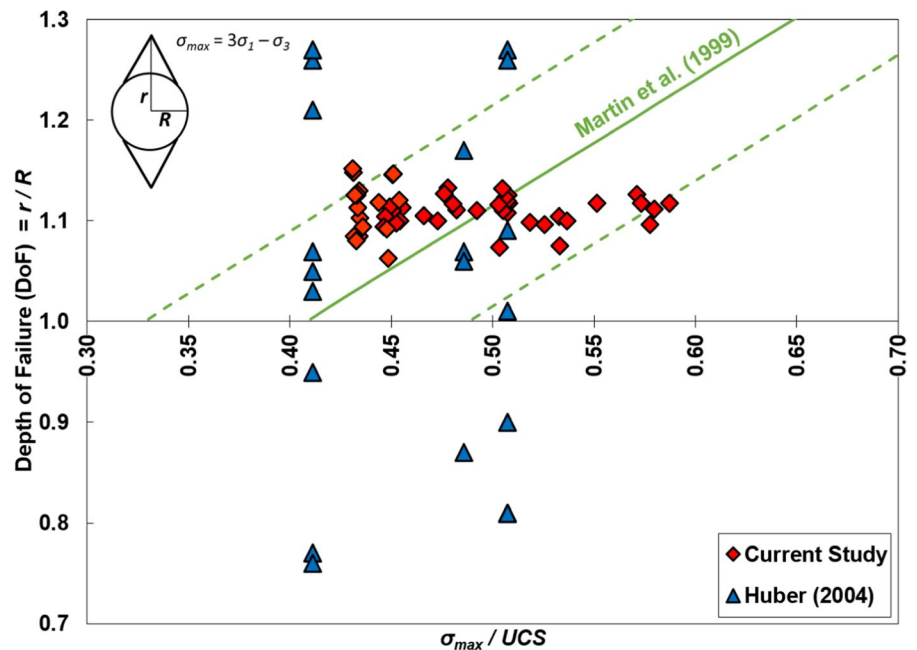

between 0.41 and 0.51. The wide DoF range relates to where scans taken, particularly where sever signs of over-break were observed in 2004 (Huber 2004). The scanning method also contributed to limiting the range of damage depth that could be assessed in each scan, since a swath of data was only captured over a few centimeters' length of the adit wall. With such a limited width of scan, this would mean that taking a single cross section plane at a given tunnel chainage could over or underestimate the average or typical depth of failure within several meters of the scan location along the adit wall. This is in contrast with the 2017 measurements which captured up to 6 m length of the adit wall in one scan. This more continuous method means that a range of overbreak depths can be assessed and averaged more accurately to remove the "noise" that a single swath scan may produce when attempting to capture the typical overbreak depth. Hence, the data was used as an average of a tunnel section, using a bi-dimensional analysis. The sampled points showed that 63% of the scanned sections did not deliver data within Martin et al (1999) empirical trends. For instance, the tunnel walls exposed to "structures parallel to the tunnel adit axis or a fractured rock mass" (Huber 2004) were also scanned, and in most cases, the resulting DoF was

lower than the empirical prediction due to the structure preventing the complete formation and propagation of new spalling fractures beyond the structure in the walls. Conversely, that data from our research captured a sphere of data to sample a representative change in the tunnel walls, given by the spalling effect along tunnel lengths of 6 m, to avoid large contrasts in DoF between consecutive tunnel scans. Therefore, the DoF results scatter from 1.06 to 1.14, on a stress-strength ratio of 0.43 to 0.59 for the data of the current study, as shown in Fig. 5.

To compare the current data with Huber's (2004), the latter was reassessed in terms of strength values, fixed at 150 MPa. Furthermore, scans were grouped to cover similar extensions of those scans from the current data (2017). Both data set were reported in terms of their Volume of Failure (VoF, see Sect. 3). Hence, the Huber (2004) scanned values were re-grouped into 6 m in tunnel lengths where possible to calculate the normalised VoF of the combined scanned sections, similar to what could be done with the newly scanned data. This gave a new data set named "Huber (2004) Modified", and it forms the base of the assessment with the time of the change in the DoF of the Bedretto adit, which is introduced in Fig. 6.

Fig. 6 Normalised Volume of Failure (VoF) for the Bedretto adit, after correction of values due to the length of monitoring sections for both the 2004 and 2017 data acquisition periods, along with Martin et al. 1999 empirical correlation. Data from 2017 were split into Zone 1A, Zone 1B and Zone 2. Indicated are also the projected fault zone of the Geren Valley and the Geren Val-ley glacier, along with the overburden depth
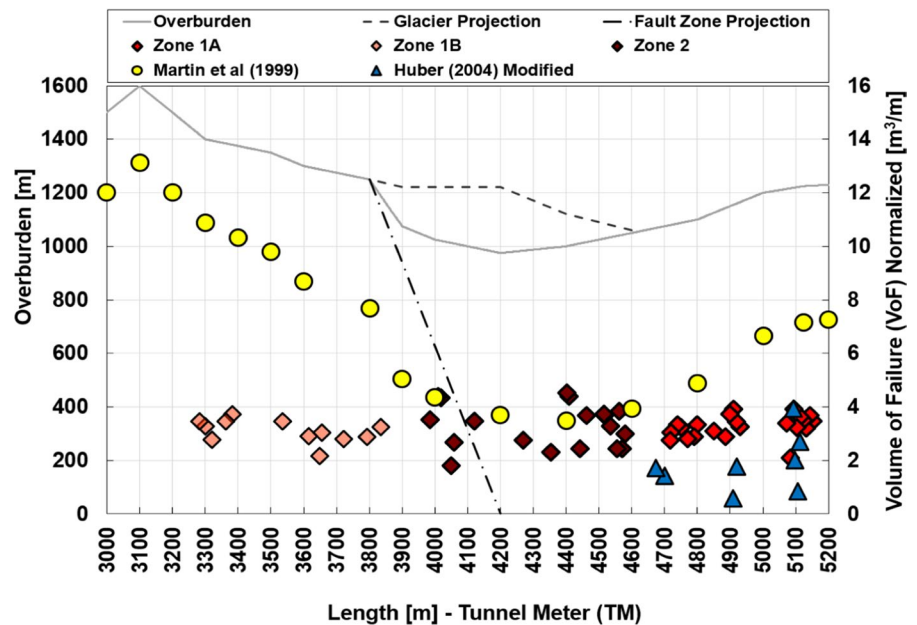
5 Analysis of the Volume of Failure

The results of the over-break depth calculations are compared in terms of the VoF between data set from 2017 and Huber (2004) Modified. Figure 6 shows the resulting VoF along the adit axis from TM-5200 to TM-3000, including other morphological elements such as the projection of a known glacier in the Geren Valley and the projection to the surface of a major fault zone observed within the adit. The left Y-axis indicates the overburden thickness in meters above the adit elevation, and the right Y-axis shows the normalised VoF per linear meter (m3/m). The maximum VoF from the empirical correlation of Martin et al. (1999) predicts is based on the local stress magnitude estimated from the over-burden depth and a K_o ratio of 0.8 with a constant UCS strength value of 150 MPa.

The calculated average values of the VoF for the current data (2017) are higher (3.23 m3/m) than the Huber (2004) Modified results (1.85 m3/m), as shown in Fig. 6. In most cases, both data sets plot below the maximum projection from Martin et al. (1999) empirical correlation, except for those sections located between TM-3985 and TM-4580 of the current data (2017). These sections are close to the Geren valley hosting a large glacier in the uppermost cirque, and a regional fault zone called

the Geren Valley fault zone. In this section of the tunnel, 10 out of 19 scanned sections were conducted, and a VoF equal approximately 80% of the projected VoF from Martin et al. (1999) correlation. Comparatively speaking, for those sections outside of the TM-3985 to TM-4580 zone, the current (2017) VoF only reaches on average 65% and Huber (2004) Modified only 38% of the maximum VoF predicted by the Martin et al. (1999) empirical correlation. This anomaly suggests that current data (2017) trends behave differently in this region, and therefore the tunnel length was divided into two different zones as follows:

- Zone 1: includes all sections located outside of TM-3985 to TM-4580. This Zone is sub-divided in Zone 1A (TM-4580 to TM-5200) with a VoF of 3.26 ± 0.4 m3/m; and Zone 1B (TM-300 to TM-3985) with a VoF of 3.09 ± 0.4 m3/m.
- Zone 1A can be compared to Huber (2004) Modified.
- Zone 2: data measured within TM-3985 to TM-4580, has a VoF of 3.27 ± 0.7 m3/m.

Even though the average predicted VoF using Martin et al. (1999) correlation is higher than that measured in the three zones (Fig. 6), the values are within the bounds when converted back to DoF values, as

Fig. 7 DoF for the Bedretto adit, considering data from 2017 and modified data from Huber (2004). The 2017 dataset has been characterised into Zones 1A, 1B and 2
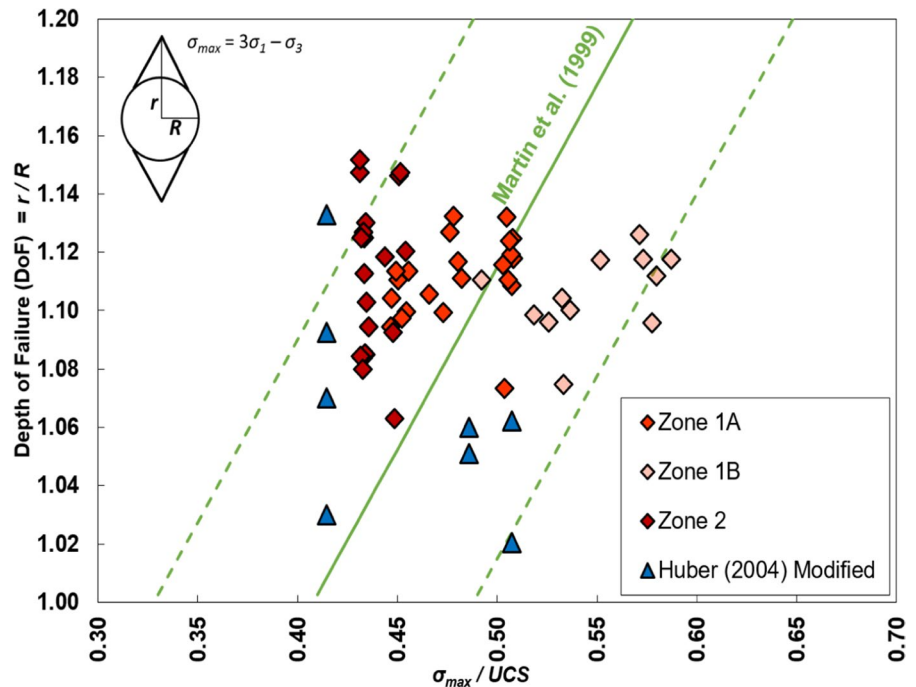
shown in Fig. 7. Martin et al. (1999) did not report the damage depths as a VoF, so some assumptions were made in conversion that could influence the results. Essentially the VoF is inscribed by a tube, rather than a circle as Martin et al. (1999) had suggested, and the average DoF along this tube is used (as described in Eq. 3). It was necessary to analyze the current data using a VoF approach since the data was collected over a 6 m length of the tunnel axis and comparing a specific tunnel meter to that of Huber's (2004) when the exact location to the centimeter is not know yields highly variable results. By averaging our collected data, it smooths the typical DoF values determined. From this point forward in the paper, the DoF values are average values per scanned section, rather than the extreme values that might exist at any given point along the adit. This has been done to generalize the data. The differences between zones are more easily observed through the DoF values, illustrated in Fig. 7. The average DoF is similar for Zone 1 (1.12 ± 0.01 m) and Zone 2 (1.12 ± 0.03 m), and both are higher than Huber (2004) Modified data (1.07 ± 0.03 m). However, the dispersion of the results (i.e. standard deviation) for Zone 2 is higher than in Zone 1. It is also shown in Fig. 7 how Zone 2's DoF data distribute in a very narrow range of stress-strength ratios. The Zone

1 values are within the expected empirical range for the Bedretto adit, except for three points plot one or below the lower boundary suggested by Martin et al. (1999) in Fig. 7. The point plotting furthest below the lower boundary is at TM-3282, at the most left extent of measurements in Fig. 6. This coincides with a sudden increase in the overburden thickness and likely a sudden change in the stress magnitude. This point is shown in Fig. 7 at the outer portion of the projection of Martin et al. (1999) correlation below the lower boundary (at a stress-strength ratio of 0.6). Zone 1A values generally plot near or above the average predicted DoF using the empirical projection.

When comparing the two time periods (2004 against 2017), the average equivalent radius has increased on average for the adit sections located between TM-4600 to TM-5113. Statistically examining the averages, in 2004, the equivalent radius was 2.25 m, and by 2017 this value had reached 2.35 m. This translates into an increase in the adit over-break volume of about 1.5 m^3/m on average. Both Figs. 6, 7 show that most of the 2004 measurements are below those from 2017. The authors have observed this increase in damage depth with time to be a progressive process. However, the driving mechanism remains elusive as many factors must be discussed.

6 Discussion

In the analysis presented above, the rock mass properties and stress state have been held constant in order to remove this as a variable between 2004 and 2017. The results have also been compared to empirical depth of spalling limits developed by Martin et al. (1999) since a reliable value CI has not yet been determined from laboratory testing. However, for discussion purposes, the results can be compared to more recent spalling prediction work of Diederichs (2007) and the semi-empirical work of Perras and Diederichs (2016) to gain further insight into the recorded spalling damage depths from the Bedretto adit. There are many aspects that could examined conceptually and discussed that influence the spalling damage depth with time. Some of these are discussed below.

6.1 Spalling Damage and Excavation Damage Zones Around Excavations

The measurements in Zone 1A from 2004 and 2017 were compared using the VoF in Fig. 8 to discuss and understand the progressive nature of spalling and slabbing in the Bedretto adit and the potential influencing factors. Zone 1A was used as it had the most overlapping measurement locations between the two time periods. The DoF was converted to VoF by rearranging Eq. (3), again to improve comparison and to average the scan results over short lengths of the adit. Both Martin et al. (1999) and Diederichs (2007) empirical DoF relationships were converted to VoF, and the stress-strength ratio was calculated using CI, with a CI threshold value defined as 44% of UCS (Perras and Diederichs 2016). Most sections for the 2004 data plot close to the empirical relations (Martin et al. 1999; Perras and Diederichs 2016). At TM-5108, with stress—strength (CI) ratio of 1.1, the VoF (0.77 m^3/m) in 2004 is approximately half of that which would be estimated by empirical correlations
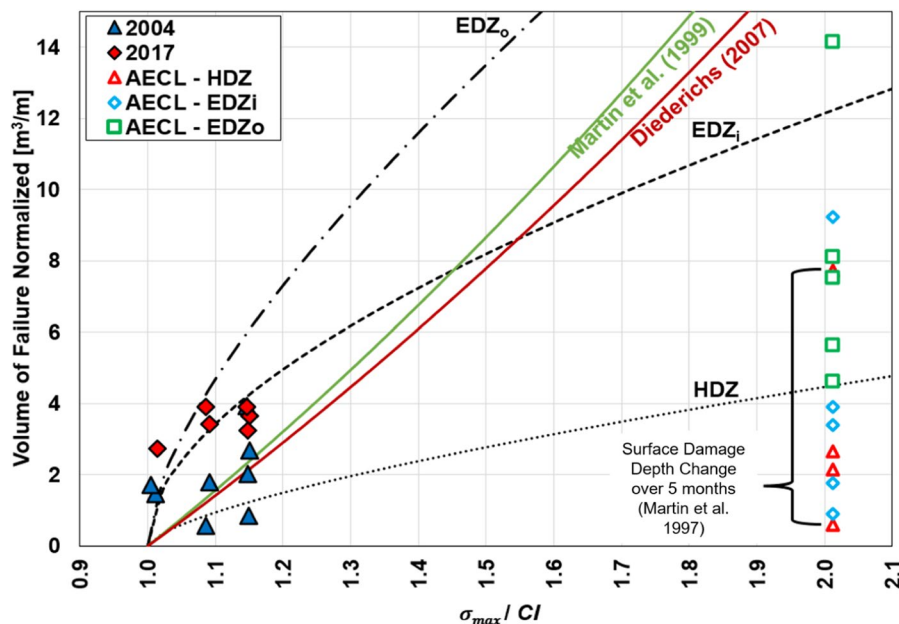

Fig. 8 Bedretto volume of failure values from 2004 and 2017 compared to the outer and inner Excavation Damage Zones (EDZo and EDZi, respectively) and the Highly Damage Zone prediction intervals, based on Perras and Diederichs (2016) and the empirical conversion of the original linear DoF from Martin et al. (1999), adjusted to a normalization by CI and the empirical relationship of Diederichs (2003). The curves were modified to represent the VoF and the data from Fig. 5 for both Huber (2004) Modified and Zone 1A (2017) measurements. Also shown is the progressive deepening of the depth of damage at the AECL underground research laboratory reported by Martin et al. (1997)

(Martin et al. 1999; Diederichs 2007). Regardless, all the 2017 values plot above the 2004 values and are well above the empirical limits. Newly formed spalled walls were still observed in 2017, as evidenced by fresh rock surfaces exposed on the tunnel walls and loose slab pieces on the floor being discoloured on one side and fresh on the other. For example, even the 2004 measurements at a low stress-strength ratio of 1.04, at adit sections TM-4920 and TM-4910, show an increase in the VoF by roughly 50%. For comparison, at a much higher stress-strength ratio, the AECL damage depth increased significantly (16 times) over five months, as indicated by the Highly Damaged Zone (HDZ) measured values reported by Martin et al. (1999) calculations and shown in Fig. 8. To the author's knowledge, these are the only two locations where progressive damage depth measurements have been reported in the literature and show increases in the damage depth with time.

Field observations from Zone 2 also indicated that some elements from the construction stage are seen more frequently in this zone, such as half-barrel drill holes in the roof (Fig. 1b), small wedge failures, and support, such as mesh and bolting in the adit walls. The latter needs to be also considered when evaluating this area due to the influence of the structural elements on the VoF values, which have been observed to reduce the spalling over-break depth. For instance, very fresh spalls have been identified during fieldwork for this study, and these are generally shallow and have small surface areas. Due to the heterogeneous geomechanical conditions and related support measures, the actual post-failure state for Zone 2 is more influenced than Zone 1. Consequently, Zone 2 has not been considered in the assessment of EDZ depths for the Bedretto adit.

Zone 1A and Zone 1B results seem to show an inverse relationship between VoF and overburden in Fig. 6. However, the plot of DoF for different stress magnitudes (at a fixed UCS or CI) shows that DoF increases while the overburden increases for both zones. This is explained using Eq. (3) and the hypothesis to average the failure by assuming a circular section, partially supported by the fact that Zone 1A has a higher VoF than Zone 1B, despite Zone 1B having thicker overburden. This difference could be explained due to clearance work and the previous state of the tunnel in Zone 1B. The latter might have created differences in the tunnel shape

and ground cover due to structural effects in this area and progressive deterioration of the rock mass quality instead of overburden stress effects. This contradiction can be observed locally in the trend of the VoF from TM-3800 to TM-3300 in Fig. 6, which decreases while the overburden increases.

One factor to consider is that the data presented by empirical methods (Martin et al. 1999; Diederichs 2007) are measured depths of damage shortly after excavation, and they represent the depth of rock that has been removed through brittle spalling and/or scaling. Similarly, the most widely cited case of brittle spalling from Canada's Underground Research Laboratory operated by AECL in the Lac du Bonnet granite is often considered by other authors doing back analysis to have developed instantaneously (see Walton and Sinha 2022), even though it developed over more than five months (Martin et al. 1997). It represents the literature's longest-lasting continuous spalling measurements around a tunnel report to the authors' knowledge. The Highly Damaged Zone (HDZ) shown in Fig. 8 is the depth of brittle spalling reported by Martin et al. (1997). If one considers the other excavation damage zones, the inner and outer Excavation Damage Zones (EDZi and EDZo, respectively—defined by Perras and Diederichs (2016) as the depths reported by Martino and Chandler (2004) and one adds the same incremental increase in the damage depth as that measured for the HDZ. The EDZi measurement increases towards the EDZi maximum depth prediction interval suggested by Perras and Diederichs (2016), which is valid for the EDZo. Given enough time, the spalled notch depth may have reached the EDZo maximum depth prediction interval of Perras and Diederichs (2016), as the data presented in this article appears to do between 2004 and 2017 (Fig. 8). This suggests that conceptually that the observed and measured continued spalling between 2004 and 2017 is related to the original micro-fracturing that was induced by the excavation process and that with time the isolated micro-cracks have grown until they begin to interact causing new spalls to detach and fall from the walls of the adit.

6.2 Strength-Degradation and Long-Term Rock Mass Behaviour

The measured changes from 2004 to 2017 in the Bedretto adit support the concept that progressive

crack growth is an ongoing process that can reach the maximum EDZo depth with enough time and no backfilling material or support to provide confinement suppression crack growth. The damage depth is limited by the high confining stress at the apex of the failure zone, as discussed by Diederichs (2007). Perhaps in the long-term, the damage depth is also limited to the extent of the original stress-induced micro-damage within the EDZo region, as evidenced by the fact that the VoF for the 2017 measurements from Bedretto and the final AECL damage zone depths are at or below the EDZo prediction limit proposed by Perras and Diederichs (2016). Conceptually, if the far-field stresses and rock mass strength remain the same, then only existing micro-cracks would be able to grow with time, and if these begin to interact with each other, then new slabs could form. Obviously, such a theory needs to be examined more rigorously. However, a long-term failure zone limit would be of practical significance for projects that involve extended de-sign time frames, which is increasingly demanded in civil engineering infrastructure tunnels and nuclear waste repository designs.

The impact of time-dependent factors is not as thoroughly studied at the tunnel scale as other more immediate rock mass responses and as such designers and researchers implicitly indicate that the impact must be small in terms of tunnel stability, but this de-pends on the final use of the excavation. With most modern excavations having mandatory support and final liners, the rock is rarely exposed, however, understanding the role of strength degradation is still critical for some underground excavations (Perras and Diederichs 2014; Paraskevopoulou 2016, 2021; Diederichs et al. 2017) where the rock may be exposed to variations in environmental factors during operation and even after closure, such as in mines and deep geological repositories (Park et al. 2022; Rutqvist 2020; Yasidu et al. 2017; Blaheta et al. 2013). The strength degradation and its relationship with water are discussed in the following sections by relating available literature to our work.

The deviation from the numerical prediction interval approach developed by Perras and Diederichs (2016) and shown in Fig. 8 can be partly due to the estimated values of UCS and the derived CI threshold. The strength values along the adit will undoubtedly vary. However, systematic measurements were not available at the time of this study. There has been a considerable variation along the adit in geological events (Huber 2004), which could cause the UCS value to deviate from the few locations where measurements were taken. Some sections have undergone ductile shearing, others minor brittle damage or faulting, and others show hydrothermal alterations. The data have been compared assuming the UCS or CI values are consistent along the length of the adit and that they have remained unchanged with time. However, recent research by Innocente et al. (2021) has shown that strength degradation can occur over time in various rock types from sedimentary to metamorphic to igneous, from soft and weak even brittle and crystalline rocks. The authors created a database from time-to-failure laboratory tests (available in the literature) on rock materials subjected to constant load and they analysed the decay of the LTS (Long-Term Strength) over time which can be represented by both a log-linear and exponential fit equation (Eqs. 6–8) Innocente et al. (2021). However, the lower bound of the LTS is the CI value under which there cannot be observed any further strength loss, where strength finds an asymptote, which is controlled by the parameter C (Eq. 7). This is agreement with Li et al. (2021a, b) who argued that in-situ stress measurements seldom exceed CI values. They also argued that strength changes are likely to occur and relate to long-term crack growth and progressive failure through a variety of mechanisms such as creep and stress relaxation that can lead ultimately to strength degradation.

$$\frac{\sigma_1}{UCS} = 0.01 \exp\left(\frac{A}{t_f^B} + C\right) \quad (6)$$

$$C = ln\left(\frac{CI}{UCS} * 100\%\right) \quad (7)$$

$$\frac{\sigma_1}{UCS} = M \ln(t_f) + N \quad (8)$$

where σ_1 is the applied stress, UCS is the ultimate compressive strength, CI is the crack-initiation stress threshold, t_f is the time to failure, M is the slope of the log-linear plot, N is the intercept of the log-linear plot at 1 s and is $\cong 1.0$, and A and B are curve fitting parameters.

In terms of external agents' effects, Zone 2 is located below the only significant topographic

depression above the Bedretto Adit: the Geren Valley. Several authors have suggested that this valley follows a regional fault zone striking SW-NE (Huber 2004; Lutzenkirchen et al. 2011; Amberg 1983). The most critical fault zone in the Bedretto adit has been observed crossing the sections between TM 4200 and 4250, presumably corresponding to this regional tectonic structure (Huber 2004; Ofterdinger et al. 2004). Based on detailed mineralogical and micro-structural analyses, it is suggested that this fault zone underwent recurrent strike-slip faulting, developing fault breccia, catalases, and fault gouges (Huber 2004). This is also supported by the Gotthard massif's seismicity, which is notably low and might be explained by the cessation of significant tectonic fault movements. In general terms, faults have a prominent influence in brittle failure which depends on the distance to the excavations typically within the Excavation Influence Zone limits (EIZ), with the effects of an increasing horizontal displacement at the tunnel walls whilst shortening of the vertical displacements on the roof of the tunnel (Huber 2004; Pan et al. 2020). Strength properties and stress conditions around this large fault zone are expected to show extreme variability and will significantly alter the peak strength of the rock, the crack growth development and stress path history, perhaps then changing the CI threshold locally.

Such variations along the length of the adit would not significantly alter the comparison from 2004 to 2017, and the authors' current understanding of the CI threshold would be that this value does not change significantly with time. However, recent research has shown that water infiltration and even changes in humidity can have a significant influence on the stiffness of the intact rock (Li et al. 2021a, b).

Water inflows and fluctuations in the environmental parameters could also lead to the degradation of the rock mass properties with time. Therefore, it may be possible that the strength used in the calculations does not accurately reflect the current conditions. For example, if the UCS or CI values were lower, the currently determined VoF would shift up to the right on the graph in Fig. 8. The unique situation in the Bedretto adit is that it has been exposed to humidity fluctuations and unsupported for a long time. So, there has been time to propagate damage and failure deeper into the rock mass. As a slab falls off, the maximum tangential stress is pushed deeper into the rock mass, causing more damage, or at least causing existing micro damage to become connected to form new slabs at the notch tip. So, one must consider that the local stress around the excavation is also changing due to the damage progression. Likewise, Eberhardt (2001) points out, this damage accumulation irreversibly changes the rock mass's strength and deformation behaviour. The influence of humidity cannot be underestimated, as work by Li et al. (2022) has demonstrated that changes in humidity from 20 to 90% can decrease an intact rock's Young's modulus by 13%, increase Poisson's ration by 130%, which can intern induce an internal stress of 24.5 MPa in a granitic rock cylinder tested in the laboratory. Although such changes and the associated stress increase is small compared to the compressive strength, estimated to be between 150 and 175 MPa, repeated fluctuations due to humidity changes even at a seasonal variation will induce fatigue with time. The situation in Bedretto is also exasperated, since every time a train passes through the Furka tunnel a pressure wave is transmitted out through the Bedretto adit. This pressure wave has been observed by the authors to increase the humidity in the northern section to close to 100%, as the tunnel completely fogs up for several minutes due to the pressure wave.

The characteristics discussed above highlight the importance of improving our understanding of the factors that influence progressive damage evolution. Climate variables can also affect crack initiation and propagation rates (Collins et al. 2018; Alciano-Olivares et al. 2021, 2023; Grechi et al. 2023), which will change the mechanical response of the rock mass progressively and, in turn, the notch formation. For in-stance, temperature fluctuation within the adit could be triggered by changes in the air's relative humidity and produce crack expansion by thermal strain in addition to hygroscopic expansion (Wang et al. 1982; Li et al. 2021a, b, 2022). In fact, under real conditions, water flow through pores and fractures can influence the rock mass's temperature even within short distances (Zhao 2014; Luo et al. 2016). This effect could lead to stress corrosion processes and long-term strength-degradation (Bielus and Lajtai 1986; Paraskevopoulou et al. 2018; Innocente et al. 2022). These time-dependent processes are currently not part of tunnel design procedures, even though they could be critical for the expected design lifetimes

of current underground construction projects. Further studies should include the use of monitoring tools to implement recursive methods to feed algorithms for deformation and structural features (Rosso et al. 2023; Xue and Li 2018; Wu et al. 2020; Luo et al. 2020), which could be also inputs for other approaches developed after Martin et al. (1999), over the last decades (Mitri 2007; Castro et al. 2012; Kaiser 2019).

6.3 Limitations of the Current Study

The present study was conducted at an opportune time with a limited budget. Three days of field work were available to conduct the LiDAR scans. Given more time and resources, the team would have conducted continuous LiDAR scanning throughout the full 5.2 km of the Bedretto adit, installed sensors to measure stress, deformation, and correlate these with climatic variations. However, the authors and through personal discussions with other researchers, needed preliminary data to determine decidedly if the observed progressive spalling over many years was indeed resulting in measurable changes in the depth of damage. Small scale spalls could be seen as freshly exposed surfaces on the adit walls during yearly visits, however, measurements had never been conducted. With the measurements presented in this paper, further studies could address the limitations of the current work.

The biggest limitation of the present study is the lack of measured intact rock properties. The empirical depth of failure approaches (Martin et al. 1999; Diederichs 2007; Perras and Diederichs 2016) all rely on a measured UCS or CI value as a primary input. Although an estimated UCS value based on point load testing was used in the present study, a more accurate measurement would give greater confidence in the findings. A single UCS value and from this an estimated CI value were used for both time periods to eliminate deviations due to using multiple strength values. However, it could be possible to conduct long-term strength degradation tests to determine if a decrease in the UCS with time can be estimated and use this trend to extrapolate the potential strength back in time. Without proper intact rock test results, changing the strength used in this preliminary study would be speculative.

Another limitation is the estimation of the maximum tangential stress around the adit. At the time of writing this article, no stress measurements in the northern section of the tunnel have been undertaken. The value reported by Gischig et al. (2020) was used in a similar manner as the strength, with a constant stress ratio being used and only changing the vertical component due to the changes in overburden. Stress has always been a challenge parameter to measure in-situ and accurate measurements along the entire length of the adit are unreasonable. However, future research will measure the stress field near the Bedretto Lab in the southern end of the adit for the PRECODE project. With a sound measurement, a regional scale model could be used to examine the variation in stress along the length of the adit and this could in turn be used to refine the depth of spalling damage. As Potyondy (2007) stated, our biggest limitation in developing numerical approaches for time-dependent rock mass behaviour is data to validate such modelling methods. The Bedretto adit represents one of the longest durations of observed spalling in the literature and with further data collected in the future will be suitable to help aid in the development of a realistic long-term brittle rock mass behavioural model.

7 Concluding Remarks

The Bedretto adit has been left primarily unsupported ever since construction finished in 1982. A field campaign in 2017 was carried out to measure the depth of damage and compare results to a previous campaign in 2004 using LiDAR scans. The results indicate that the DoF in 2004 was on average 1.07 ± 0.03 m and in 2017 averaged 1.12 ± 0.03. If the maximum range is examined, this is an increase of 0.1 m in 13 years. DoF values were compared with linear correlation of Martin et al. (1999), which was found to overpredict the measured DoF from the Bedretto adit. Notable variations in the 2004 and 2017 DoF results indicated that specific locations can influence the measured results. Since the exact locations of Huber's (2004) scans were not known, the authors used a unique VoF approach to facilitate comparison, with variations being less using a volumetric approach or VoF presented in this paper. Using the VoF it was found that in 2004 it was 1.9 m^3/m and in 2017 3.2 m^3/m, which represents an increase of 1.3 m^3/m.

A comparison to excavation damage zones reported by Perras and Diederichs (2016) indicated that the current DoF aligns better with the EDZo prediction interval which represents a region of isolated micro-cracks rather than failed material. This suggests that conceptually that the observed and measured continued spalling between 2004 and 2017 is related to the original micro-fracturing that was induced by the excavation process and that with time the isolated micro-cracks have grown until they begin to interact causing new spalls to detach and fall from the walls of the adit. The observed damage was noticed by the authors during yearly site visits and was confirmed by comparison of the LiDAR scans from the two measurement campaigns. Such a long period of spalling, resulting at least conceptually in crack propagation over a 41-year period, has not been documented by any other authors (to the author's knowledge) Over a multi-year period. This observation should be a key consideration for future underground excavations that will have long design lifetimes and may experience spalling. Further research is needed to understand better the contributing factors that have influenced the progressive damage development in the Bedretto adit and identify the fundamental mechanisms that drive the damage processes with time.

Data Availability Enquiries about data availability should be directed to the authors.

Declarations

Conflict of interest The authors declare no competing interests related to data acquisition, analysis and discussion derived from the present work; involving either conflict of interests or breaching the Code of Ethics from their individual institutions.

References

Alcaíno-Olivares R (2017) Monitoring the influence of rock moisture on long-term crack growth in the Bedretto Tunnel, Switzerland. [Unpublished master's thesis]. University of Leeds, Leeds, United Kingdom

Alcaíno-Olivares R, Leith K, Ziegler M, Perras MA (2021) Thermo-mechanical fatigue cracking of the bedrock on an island in the Baltic Sea. In: Proceedings of the GeoNiagara 2021, Niagara Falls, ON, Canada, 26–29 Sept 2021

Alcaíno-Olivares R, Ziegler M, Bickel S, Leith K, Perras MA (2023) Monitoring and modelling the thermally assisted deformation of a rock column above tomb KV42 in the Valley of the Kings. Egypt Rock Mech Rock Eng 56:8255–8288

Amberg R (1983) Design and construction of the Furka Base Tunnel. Rock Mech Rock Eng 16(4):215–231

Amberg R, Sala A (1984) Shotcrete as permanent lining for the Furka Base Tunnel. Rock Mech Rock Eng 17(1):1–14

Andresson JC, Martin CD (2009) The Aspo pillar stability experiment: part I—experiment design. Int J Rock Mech Min Sci 46(5):865–878

Askaripour M, Saeidi A, Rouleau A, Mercier-Langevin P (2022) Rockburst in underground excavations: a review of mechanisms, classification, and prediction methods. Undergr Space 7(4):577–607

Aujmaya L, Vazaios I, Paraskevopoulou C (2022) Assessing the tunnel stability in brittle rocks based on strain bursting assessment. In: Proceedings of EUROCK 2022 on rock and fracture mechanics in rock engineering and mining, 12–15 Sept 2022, Espoo, Helsinki-region, Finland

Barton N, Shen B (2017) Risk of shear failure and extensional failure around over-stressed excavations in brittle rock. J Rock Mech Geotech Eng 9(2):210–225

Bielus LP, Lajtai EZ (1986) Stress corrosion cracking of Lac du Bonnet granite in tension and compression. Rock Mech Rock Eng 19(2):71–87

Blaheta R, Byczanski P, Čermák M, Hrtus R, Kohut R, Kolcun A, Malík J, Sysala S (2013) Analysis of Äspö pillar stability experiment: continuous thermo-mechanical model development and calibration. J Rock Mech Geotech Eng 5(2):124–135

Boon CW (2022) An instability line for spalling around circular openings and the limiting effects of scale. Rock Mech Rock Eng 55:5759–5772

Brantut N, Heap MJ, Baud P, Meredith PG (2014) Rate- and strain-dependent brittle deformation of rocks. J Geophys Res Solid Earth 119(3):1818–1836

Castro LAM, Bewick RP, Carter TG (2012) An overview of numerical modelling applied to deep mining. In: Azevedo R (ed) Innovative numerical modelling in geomechanics. CRC Press, Taylor & Francis, London, pp 393–414

Chiwara J, Vazaios I, Paraskevopoulou C, (2023) The influence of brittle failure and its impact on face stability in high-stress tunnelling conditions. In: Schubert & Kluckner (eds) Proceedings of ISRM 2023 15th international ISRM Congress 2023 & 72nd geomechanics colloquium in challenges in rock mechanics and rock engineering, 2023 Oct, Salzburg, Austria

Collins BD, Stock GM, Eppes MC, Lexiw SW, Corbett SC, Smith JB (2018) Thermal influences on spontaneous rock dome exfoliation. Nat Commun 9(762):1–13

Diederichs MS (2003) Rock fracture and collapse under low confinement conditions. Rock Mechanics and Rock Engineering 36(5):339–381

Diederichs MS (2007) The 2003 Canadian Geotechnical Colloquium: mechanistic interpretation and practical application of damage and spalling prediction criteria for deep tunnelling. Can Geotech J 44(9):1082–1116

Diederichs MS, Carter T, Martin CD (2010) Practical rock spall prediction in tunnels. In: Proceedings of ITA World tunnel congress, Vancouver, Canada 14–20 May 2010

Diederichs MS, Day JJ, Ghazvinian E, Perras MA, Paraskevopoulou C, Walton G (2017) Progressive brittle damage processes and failure in rock. Keynote Lecture in the Progressive Failure and Long-term Strength Degradation of Brittle Rocks. In: Proceedings of the progressive rock failure 2017 (ISRM), Ascona, Switzerland, Conference, June 2017, Ascona, Switzerland, 5–9 June 2017

Duan K, Ji Y, Wu W, Kwok CY (2019) Unloading-induced failure of brittle rock and implications for excavation induced strain burst. Tunn Undergr Space Technol 84:495–506

Eberhardt E (2001) Numerical modelling of three-dimension stress rotation ahead of an advancing tunnel face. Int J Rock Mech Min Sci 38(4):499–518

Gischig VS, Giardini D, Amann F et al (2020) Hydraulic stimulation and fluid circulation experiments in underground laboratories: stepping up the scale towards engineered geothermal systems. Geomech Energy Environ 24:100175

Grechi G, D'Angio D, Salvatore M (2023) Analysis of thermally induced strain effects on a jointed rock mass through microseismic monitoring at the Acuto Field Laboratory (Italy). Appl Sci 13:2489

Guo J, Zhang H, Sun F, Shi X, Zhu B, Guo P (2023) Numerical simulation study of catastrophe process for structural-slip rockburst. Geotech Geol Eng 41:4007–4022. https://doi.org/10.1007/s10706-023-02501-w

Huber B (2004) Stress-induced fractures in the deep-seated Bedretto tunnel: their geological and geomechanical reasons [Unpublished diploma's dissertation]. Swiss Federal Institute of Technology Zurich, Zürich, Switzerland

Innocente J, Paraskevopoulou C, Diederichs MS (2021) Estimating the long-term strength and time-to-failure of brittle rocks laboratory testing. Int J Rock Mech Min Sci 174:104900

Innocente J, Paraskevopoulou C, Diederichs MS (2022) Time-dependent model for brittle rocks considering the long-term strength determined from lab data. Mining 2:463–486. https://doi.org/10.3390/mining2030025

Jiang Q, Wang B, Feng XT, Fan QX, Wang Z, Pei SF, Jiang S (2019) In situ failure investigation and time-dependent damage test for columnar jointed basalt at the Baihetan left dam foundation. Bull Eng Geol Env 78:3875–3890

Kaiser PK (2019) From common to best practices in underground rock engineering. In Proceedings of 14th ISRM Congress: rock mechanics for natural resources and infrastructure development, Brazil, Argentina, Paraguay, 13th Sept 2019

Keller F, Schneider TR (1982) Geologie und Geotechnik. Schweizer Ingenieur Und Architekt 24(82):512–520

Keller F, Wanner H, Schneider TR (1987) Geologischer Schlussbericht Gotthard-Strassentunnel. Schweizerischen Geotechnischen Kommission, Bern

Keneti A, Sainsbury B-A (2020) Development of a comparative index for the assessment of the severity of violent brittle faliures around underground excavations. Eng Geol 270:105596

Li Y, Su G, Pang J, Liu C, Zhang Q, Yang X (2021a) Mechanism of structural-slip rockbursts in Civil Tunnels: an experimental investigation. Rock Mech Rock Eng 54:2763–2790. https://doi.org/10.1007/s00603-021-02429-8

Li Y, Leith K, Perras MA, Loew S (2021b) Digital image correlation-based analysis of hygroscopic expansion in Herrnholz granite. Int J Rock Mech Min Sci 146:104859

Li Y, Leith K, Perras MA, Loew S (2022) Effect of ambient humidity on the elasticity and deformation of unweathered granite. J Geophys Res Solid Earth 127(11):e2022JB024004

Luo S, Zhao Z, Peng H, Pu H (2016) The role of fracture surface roughness in macroscopic fluid flow and heat transfer in fractured rocks. Int J Rock Mech Min Sci 87:29–38

Luo Y, Gong FQ, Li XB, Wang SY (2020) Experimental simulation investigation of influence of depth on spalling characterics in circular hard rock tunnel. J Central South Univ 27(3):891–910

Lützenkirchen V, Loew S (2011) Late Alpine brittle faulting in the Rotondo granite (Switzerland): deformation mechanisms and fault evolution. Swiss J Geosci 104(1):31–54

Martin CD, Christiansson R (2009) estimating the potential for spalling around a deep nuclear waste repository in crystalline rock. Int J Rock Mech Min Sci 46(2):219–228

Martin CD, Kaiser PK, McCreath DR (1999) Hoek-Brown parameters for predicting the depth of brittle failure around tunnels. Can Geotech J 36(1):136–151

Martin CD, Read RS, Martino JB (1997) Observations of brittle failure around a circular test tunnel. Int J Rock Mech Min Sci 34(7):1065–1073

Martino JB, Chandler NA (2004) Excavation-induced damage studies at the underground research laboratory. Int J Rock Mech Min Sci 41(8):1413–1426

Mitri HS (2007) Assessment of horizontal pillar burst in deep hard rock mines. Int J Risk Assess Manag 7(5):695–707

Nara Y, Nakabayashi R, Maruyama M, Hiroyoshi N, Yoneda T, Kaneko K (2014) Influences of electrolyte concentration on subcritical crack growth in sandstone in water. Eng Geol 179:41–49

Ofterdinger US, Balderer W, Loew S, Renard P (2004) Environmental isotopes as indicators for ground water recharge to fractured granite. Ground Water 42(6/7):868–879

Ortlepp WD, Stacey TR (1994) Rockburst mechanisms in tunnels and shafts. Tunn Undergr Space Technol 9(1):59–65

Pan PZ, Miao S, Wu Z, Feng XT, Shao C (2020) Laboratory observation of spalling process induced by tangential stress concentration in hard rock tunnel. Int J Geomech 20(3):04020011

Paraskevopoulou C (2016) Time-dependency of rock and implications associated with tunnelling. [Doctoral thesis] Queen's University, Kingstone, Ontario, Canada

Paraskevopoulou C (2021) Time-dependent behavior of rock materials. In: Lwisa E, Arman H (eds) Engineering geology. IntechOpen, Rijeka, p 134

Paraskevopoulou C, Perras MA, Diederichs MS, Amann F, Loew S, Lam T (2015a) Long-term static load laboratory testing behaviour of different rock types. In: Proceedings of the 68th Canadian geotechnical symposium GeoQuebec on challenges from North to South, 2015 Sept, Quebec, Canada

Paraskevopoulou C, Perras MA, Diederichs MS, Amann F, Loew S, Lam T (2015b) Observations for the long-term behaviour of carboniferous limestone rocks based on laboratory testing. In: Proceedings of the EUROCK 2015 future development of rock mechanics—64th Geomechanics Colloqium, 2015 Oct, Salzburg, Austria

Paraskevopoulou C, Perras MA, Diederichs MS, Amann F, Loew S, Lam T, Jensen M (2017) The three stages of stress-relaxation—Observations for the long-term behaviour of rocks based on laboratory testing. J Eng Geol 216:56–75

Paraskevopoulou C, Perras MA, Diederichs MS, Loew S, Lam T, Jensen M (2018) Time-dependent behaviour of brittle rocks based on static load laboratory testing. J Geotech Geol Eng 36:337–376

Park JW, Lee YK, Park C, Kim CM (2022) Crack initiation and propagation thresholds of Hwangdeung granite under elevated temperature. Geosci J 26(6):715–729

Perras MA, Diederichs MS (2014) A review of the tensile strength of rock: concepts and testing. Geotech Geol Eng 32(2):525–546

Perras MA, Diederichs MS (2016) Predicting excavation damage zone depths in brittle rocks. J Rock Mech Geotech Eng 8(1):60–74

Potyondy D (2007) Simulating stress corrosion with a bonded-particle model for rock. Int J Rock Mech Min Sci 44:677–693

Rosso MM, Marasco G, Aiello S, Aloisio A, Chiaia B, Marano GC (2023) Convolutional networks and transformers for intelligent road tunnel investigations. Comput Struct 275:106918

Rutqvist J (2020) Thermal management associated with geologic disposal of large spent nuclear fuel canisters in tunnels with thermally engineered backfill. Tunn Undergr Space Technol 102:103454

Walton G, Sinha S (2022) Challenges associated with numerical back analysis in rock mechanics. J Rock Mech Geotech Eng 14(6):2058–2071

Wang HF, Bonner BP, Carlson SR, Kowallis B, Heard HC (1982) Thermal stress cracking in granite. J Geophys Res Solid Earth 94(B2):1745–1758

Wu Z, Wu S, Cheng Z (2020) Discussion and application of a risk assessment method for spalling damage in a deep hard-rock tunnel. Comput Geotech 124:103632

Wu S, Han S, Wang Y, Zhu Z, Chen L, Nian Y (2023) Assessment and prediction of rockburst risk zones under different structural plane shapes. Geotechn Geol Eng 41:4395–4414. https://doi.org/10.1007/s10706-023-02522-5

Xue Y, Li Y (2018) A fast detection method via region-based fully convolutional neural networks for shield tunnel lining defects. Comput Aided Civ Infrast Eng 33(8):638–654

Xue Y, Xu T, Heap MJ, Meredith PG, Mitchell TM (2023) Time-dependent cracking and brittle creep in macrofractured sandstone. Int J Rock Mech Min Sci 162:105305

Yasidu UM, Fujii Y, Fukuda D, Kodama JI, Maneya G (2017) Effect of humidity on tensile strength of rocks in selected underground coal mines in Malawi. In: Proceedings of 51st American Rock Mechanics Association 2017, San Francisco, CA, United States, 26–27 June 2017

Zhang C, Feng XT, Zhou H, Qiu S, Wu W (2012) Case histories of four extremely intense rockbursts in deep tunnels. Rock Mech Rock Eng 45(3):275–288

Zhang Z, Chen F, Li N, He M (2019) Influence of fault on the surrounding rock stability for a mining tunnel: distance and tectonic stress. Adv Civ Eng 1:12

Zhang W, Feng XT, Xiao YX, Feng GL, Yao ZB, Hu L, Niu WJ (2020a) A rockburst intensity criterion based on the Geological Strength Index, experiences learned from a deep tunnel. Bull Eng Geol Environ 79:3585–3603. https://doi.org/10.1007/s10064-020-01774-2

Zhang S, Ma T, Tang CA, Jia P, Wang YC (2020b) Microseismic monitoring and experimental study on mechanism of delayed rockburst in deep-buried tunnels. Rock Mech Rock Eng 53(16):2771–2788

Zhao Z (2014) On the heat transfer coefficient between rock fracture walls and flowing fluid. Comput Geotech 59:105–111

Zhao J, Feng X, Guo H, Hu Y, Chen G, Yang C (2022) Time-dependent failure characteristics of excavated rock masses in deep buried engineering: a field case and experimental study. Bull Eng Geol Env 81:520

Zhoa G, Wang D, Shi L, Wang S (2023) Influences of EDZ and cross-section shapes on spalling failure depth of noncircular tunnels in gneissic granite. Geotechn Geol Eng 41:91–105. https://doi.org/10.1007/s10706-022-02264-w

Zhou H, Meng F, Zhang C, Hu D, Yang F, Lu J (2015) Analysis of rockburst mechanisms induced by structural planes in deep tunnels. Bull Eng Geol Environ 74:1435–1451. https://doi.org/10.1007/s10064-014-0696-3